XVI International Conference on Computational Plasticity. Fundamentals and Applications
COMPLAS 2021
E. Oñate, D. Peric, M. Chiumenti and Eduardo de Souza Neto (Eds)

EFFECT OF LODE PARAMETER AND STRESS TRIAXIALITY ON THE EFFECTIVE PLASTIC YIELD PROPERTIES OF TRIPLY PERIODIC IWP LIGAMENT-BASED MINIMAL SURFACE

Nareg Baghous[a,b,*], **Imad Barsoum**[a,b,†] **and Rashid K. Abu Al-Rub**[a,b,††]

(a) Advanced Digital & Additive Manufacturing (ADAM) Center, Khalifa University of Science and Technology, 127788, Abu Dhabi, United Arab Emirates.

(b) Department of Mechanical Engineering, Khalifa University of Science and Technology, 127788, Abu Dhabi, United Arab Emirates.

† Email: imad.barsoum@ku.ac.ae, Web page: http://www.ku.ac.ae
†† Email: rashid.abualrub@ku.ac.ae, Web page: http://www.ku.ac.ae

Key words: Computational Plasticity, Yield Surface, Effective Yield Strength, TPMS, Lode.

Abstract. *Due to the advancements in additive manufacturing and increased applications of additive manufactured structures, it is essential to fully understand both the elastic and plastic behavior of cellular materials, which include the mathematically-driven triply periodic minimal surfaces (TPMS). The elastic and plastic behaviors have been well established for many TPMS structures. These structures are however rather computationally expensive to model explicitly when used in meta-materials and hence the need to develop an accurate yield function in order to model their plastic behavior in a homogenized approach. In this study, the effect of different loading conditions is numerically investigated on the effective yield strength of IWP ligament-based (IWP-L) TPMS. The simulations are based on a single unit cell of IWP-L under periodic boundary conditions, assuming an elastic-perfectly plastic material, for relative densities ranging from 7% to 28%. In order to define and account for the different loading conditions, the Lode parameter (L) is used. The effect of L is studied over a range of stress triaxialities (T) to understand the effect of both L and T on the effective yield strength. The results show that the effective yield surface for IWP-L should be characterized by T and L, and that the effect of these parameters is similar for the entire range of relative densities considered. In terms of T, yield strength is higher under lower T values, while in terms of L, yield strength is highest for L = 0 (shear loading) and is least for L = ± 1. It is found that the yield strength values are similar for L = +1 (compression) and L = -1 (tension), indicating similar yielding behavior under compression and tension loading conditions, respectively. These findings will guide the development of a yield function that takes into consideration the effect of both T and L to accurately predict the yielding of TPMS based cellular meta-materials.*

1 INTRODUCTION

Over recent years, there has been a lot of interest in the fabrication of architected cellular materials, due to the advancements in additive manufacturing techniques. These materials can provide the opportunity for an extraordinary combination of material properties that can satisfy

different applications. Within this category of materials, the mathematically-driven triply periodic minimal surfaces (TPMS) have shown promising mechanical properties and performance compared to other cellular structures [1, 2, 3]. TPMS are surfaces that locally minimize the surface area of the boundary designated so that the average curvature at each point on the surface is zero [4, 2]. The elastic and plastic behaviors of these structures have been extensively investigated [1, 5, 3, 6, 7], but it is computationally expensive to model them explicitly when used in meta-materials and hence the need to develop an accurate yield function in order to model their plastic behavior in a homogenized approach. It is interesting to note that very few attempts have been made to come up with a yield function for cellular materials generally. Deshpande and Fleck [8] developed a yield function for metallic foams, in terms of hydrostatic stress and effective stress, which shows good agreement with the experimental results. Also, McElwain et al. [9] numerically developed a yield function for porous materials with cubic symmetry, that is an extension to the Gurson-Tvergaard-Needleman yield criterion. In this case, the yield criterion is a function of hydrostatic stress, equivalent stress and void fraction.

In terms of bulk materials, it has been proven that a material stress state is best characterized by both the stress triaxiality T and the Lode parameter L [10, 11]. Thus, it is important to investigate the effect of L on the yield surface of cellular materials to obtain a yield function that accurately represents the behavior of such materials. T is simply defined as

$$T = \frac{\sigma_h}{\sigma_e} \tag{1}$$

where σ_h and σ_e are the hydrostatic and the Von-Mises equivalent stresses, respectively, while L is defined as

$$L = \frac{2\sigma_2 - \sigma_1 - \sigma_3}{\sigma_1 - \sigma_3} \tag{2}$$

where $\sigma_1 \geq \sigma_2 \geq \sigma_3$ are the principal stresses. L ranges from –1 to +1, where L = –1 corresponds to the axisymmetric tensile condition, L = 0 corresponds to the generalized shear or plane strain condition and a Lode value of L = +1 corresponds to the generalized compression or equibiaxial tension condition. In this paper, the effect of the T and L are investigated on the yield surface of the IWP ligament-based (IWP-L) TPMS, shown in Figure 1(a).

2 FINITE ELEMENT MODELLING

The IWP-L is constructed using MSLattice software [12], which is a software that can be used to generate the surface geometries of various types of lattices. Then, the surface geometry generated by MSLattice is input into HyperMesh software in HyperWorks suite by Altair [13], where initially a surface mesh is created and then a 3D solid mesh is created from the surface geometry. HyperMesh creates the 3D solid mesh in a very efficient way compared to the standard method of converting surface geometries to solid geometries. At this point, the structure is ready to be analyzed by any finite element analysis software. In this study, the finite

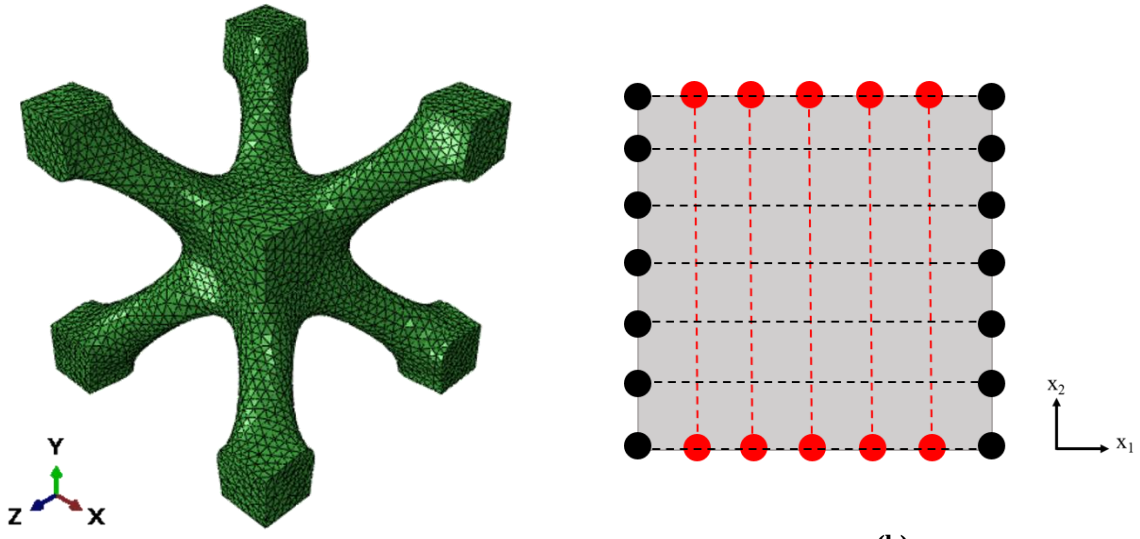

(a) **(b)**

Figure 1: (a) IWP Ligament based TPMS. (b) Periodic boundary conditions in two-dimensions

element analysis is performed using Abaqus/CAE [14], on one unit cell of IWP-L under periodic boundary conditions (PBC), which in this study is the representative volume element (RVE). The PBC is typically used to capture the bulk response of the entire cellular structure, by imposing a displacement constraint that connects each node on a surface to its corresponding node on the opposite surface of the RVE. Figure 1(b) demonstrates the concept of the PBC in two-dimensions, where each circle represents a surface node on the RVE. The black points on the x_1 faces are constrained together, while the red points on the x_2 faces are constrained together, with eq. (3).

The PBC is applied on the IWPL unit cell with 10-node quadratic tetrahedral elements (C3D10), by using a micromechanics plugin for Abaqus/CAE [15] developed by Dassault Systémes, which constraints the unit cell by

$$u_i\left(x_j + p_j^{\alpha}\right) = u_i\left(x_j\right) + \langle\frac{\partial u_i}{\partial x_j}\rangle\, p_j^{\alpha} \tag{3}$$

where u_i is the displacement vector component, x_j is the coordinate, p_j^{α} is the α^{th} vector of periodicity and $\langle\frac{\partial u_i}{\partial x_j}\rangle$ is the far-field displacement gradient applied as boundary conditions at the far-field reference nodes. Linear elastic-perfectly plastic isotropic material is assigned to the model, with the following bulk material properties: Poisson's ratio ν of 0.3, Young's modulus E of 200 GPa and yield strength σ_Y of 300 MPa. Ten-node quadratic tetrahedral elements are used on several relative densities of the IWP-L, which are 7%, 13%, 18% and 28%, with 27460, 24900, 27400 and 31300 number of elements, respectively. Note that the relative density $\bar{\rho}$ is defined as the ratio between the solid volume and the unit cell volume.

In order to capture the effect of T and L, each simulation should be driven at a constant value of T and L, by controlling the value of the concentrated forces used to drive the model, according to the following equations

$$\rho_n = \frac{3T\sqrt{3+L^2}+2L}{3T\sqrt{3+L^2}-4L} \tag{4}$$

$$\rho_s = \frac{3\sqrt{1-L^2}}{3T\sqrt{3+L^2}-4L} \tag{5}$$

where $\rho_n = \frac{\Sigma_{22}}{\Sigma_{11}} = \frac{\Sigma_{33}}{\Sigma_{11}}$ and $\rho_s = \frac{\Sigma_{12}}{\Sigma_{11}}$ [16]. Note that Σ_{ij} represents the components of the macroscopic Cauchy stress tensor acting on the unit cell, which is discussed in the following section. The values of *L* considered are ±1, ±0.8, ±0.6, ±0.5, ±0.4, ±0.2, ±0.1, 0, and for each of these *L* values, the following *T* values are considered: ±2.0, ±1.5, ±1.0, ±0.75, ±0.5, ±1/3, 0, for a total of 780 simulations for the four relative densities considered.

3 HOMOGENIZATION OF RVE

In order to capture the macroscopic effective properties of a cellular material structure from its RVE, a volume integration homogenization technique is used to calculate these properties. Thus, in order to quantify the yield strength of the TPMS structure, the effective yield strength of the IWP-L is obtained from the macroscopic effective Cauchy stress – macroscopic effective true strain response of the IWP-L unit cell, in a similar procedure as the one followed by [16]. The macroscopic effective Cauchy stress is calculated as

$$\Sigma_e = \frac{1}{\sqrt{2}}\sqrt{(\Sigma_{11}-\Sigma_{22})^2+(\Sigma_{22}-\Sigma_{33})^2+(\Sigma_{33}-\Sigma_{11})^2+6(\Sigma_{12}^2+\Sigma_{23}^2+\Sigma_{31}^2)} \tag{6}$$

where the macroscopic Cauchy stress $\boldsymbol{\Sigma}$ is equal to the volume average of the Cauchy stress $\boldsymbol{\sigma}$ acting on the unit cell. However, it has been shown that this volume average equals to the summation of the nodal reaction forces F_i^R on each face divided by the corresponding cross-sectional current area *A*

$$\Sigma_{ij} = \frac{1}{V}\int_V \sigma_{ij}\, dV = \frac{\sum_i^N F_i^R}{A} \tag{7}$$

where V and N stand for the RVE volume and the number of nodes at each boundary where the boundary conditions are applied, respectively [1, 17]. The macroscopic effective true strain E_e is simply calculated from the macroscopic effective strain ε_e

$$E_e = \ln(1+e_e) \tag{8}$$

where

$$\varepsilon_e = \int \sqrt{\frac{2}{3}\boldsymbol{D}':\boldsymbol{D}'}\,dt \tag{9}$$

and tensor $\boldsymbol{D}$ in eq. (9) represents the volume average of the rate of deformation tensor, which can be calculated from the volume average of the deformation gradient. The effective yield strength is evaluated from the effective stress - strain response by using the 0.2% strain offset method, as shown in Figure 2(a).

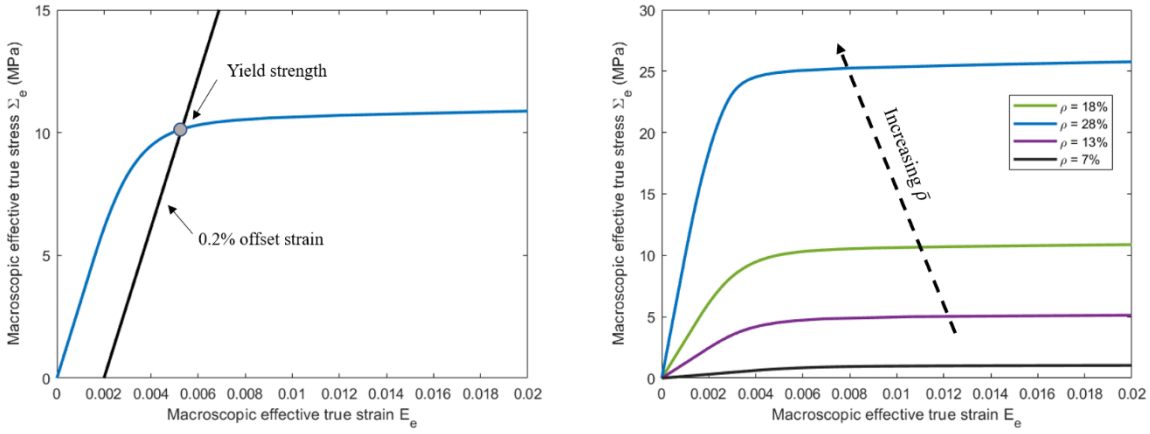

(a) **(b)**

Figure 2: (a) Method used to evaluate the yield strength from the effective true stress-strain response. (b) Effect of relative density of IWP-L on the yield strength of IWP-L at L = -1 and T = 1/3 (uniaxial tension)

4 RESULTS AND DISCUSSION

To show the effect of the relative density of the RVE on the effective properties of the TPMS structure, the stress-strain response of the four relative densities is presented in Figure 2(b), for the same T and L values. As expected, the higher the relative density, the higher the yield strength. Moreover, to understand how L and T affect the deformation of the RVE, Von-Mises equivalent stress contour plots of $\bar{\rho}$ = 18% at the increment of yielding are presented in Figure 3, for combinations of L = 0, ±1 and T = 0, ±1. The contour plots show the location of maximum Von-Mises stress and the yielding behavior under different L and T combinations, at a scale factor of x50.

The entire set of results initially are presented in Figure 4 as a two-dimensional surface of normalized yield strength and L, at constant T, where each line represents a constant T value. Note that only some T values are included and the data points have been omitted to have a comprehensible figure. All normalizations in this study are done with the yield strength of the bulk material (300 MPa). In terms of L, the 2D yield surfaces clearly show that the TPMS structure has the highest effective yield strength when L = 0. In Figure 5, the normalized yield strength is plotted versus the normalized hydrostatic stress σ_h for constant L values for $\bar{\rho}$ = 18%. σ_h is calculated from T by eq. (1), and is used instead of T, as it gives a smoother yield surface and is more commonly used than T, to represent yield surfaces. This figure shows that the highest effective yield strength is when σ_h = 0, which is the case of T = 0. The condition of T = 0 at L = 0 is the one of pure shear, which means that the IWP-L has the largest yield strength when it is loaded in pure shear. Furthermore, there is a symmetry across L, which indicates that the IWP-L TPMS yields similarly in tension (L = -1) and compression (L = +1). Moreover, it is worth noting that when T = ±2, the effect of L subsides and it looks like T becomes the dominant variable in yielding when T > 2 and T < -2. To represent the effect of all variables into one surface, a three-dimensional yield surface is constructed for each relative density, in terms of the effective yield strength, Lode parameter L and hydrostatic stress σ_h, as shown in Figure 6.

These results indicate that the analytical form of the yield surface of TPMS structures, and probably other cellular structures, must be dependent on the hydrostatic pressure σ_h, Lode parameter L and relative density of the structure, at the very least.

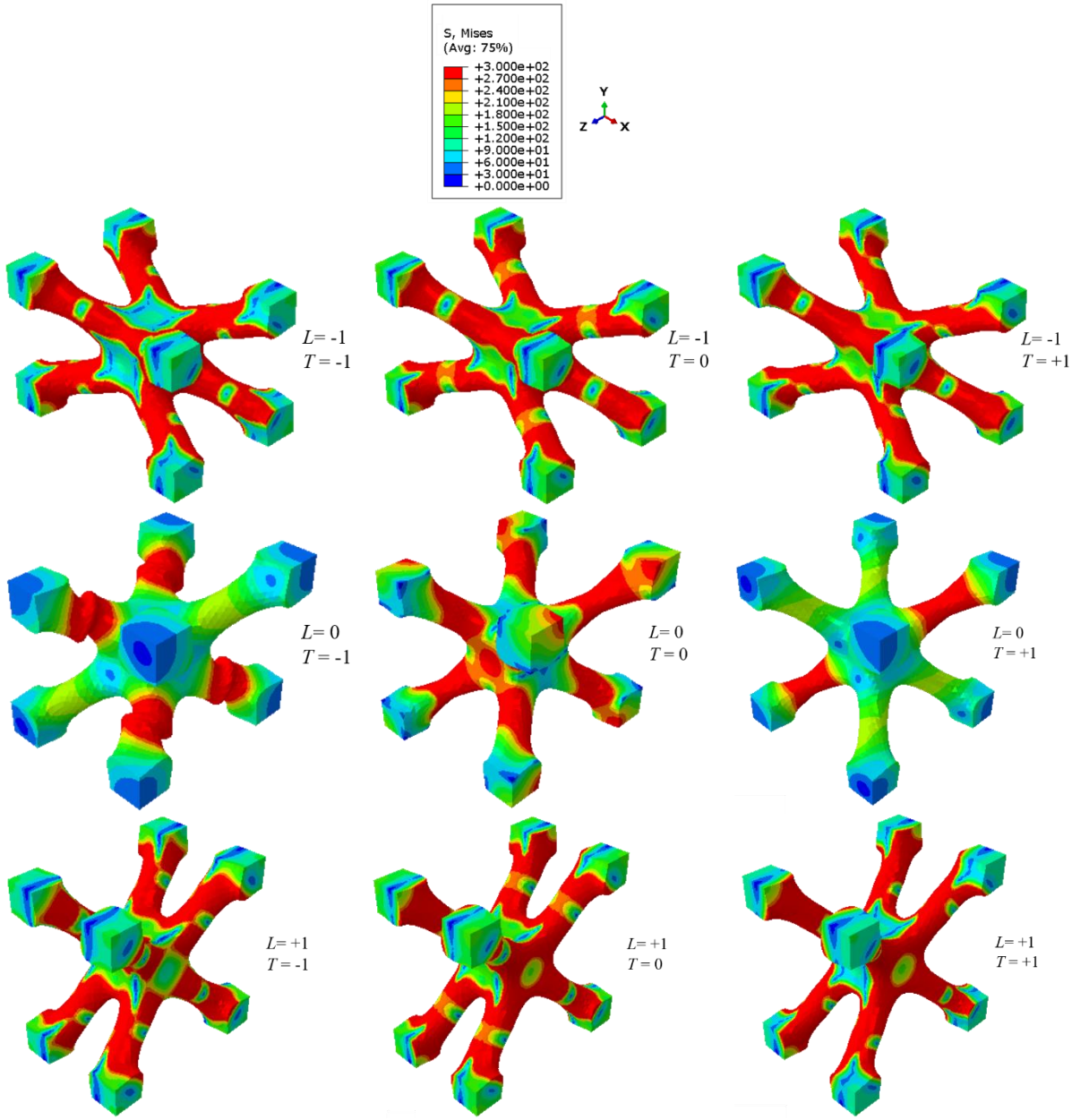

Figure 3: Von-Mises equivalent stress contour plots at the increment of yielding for $\bar{\rho}$ = 18% with x50 magnification scale factor, at different L and T combinations

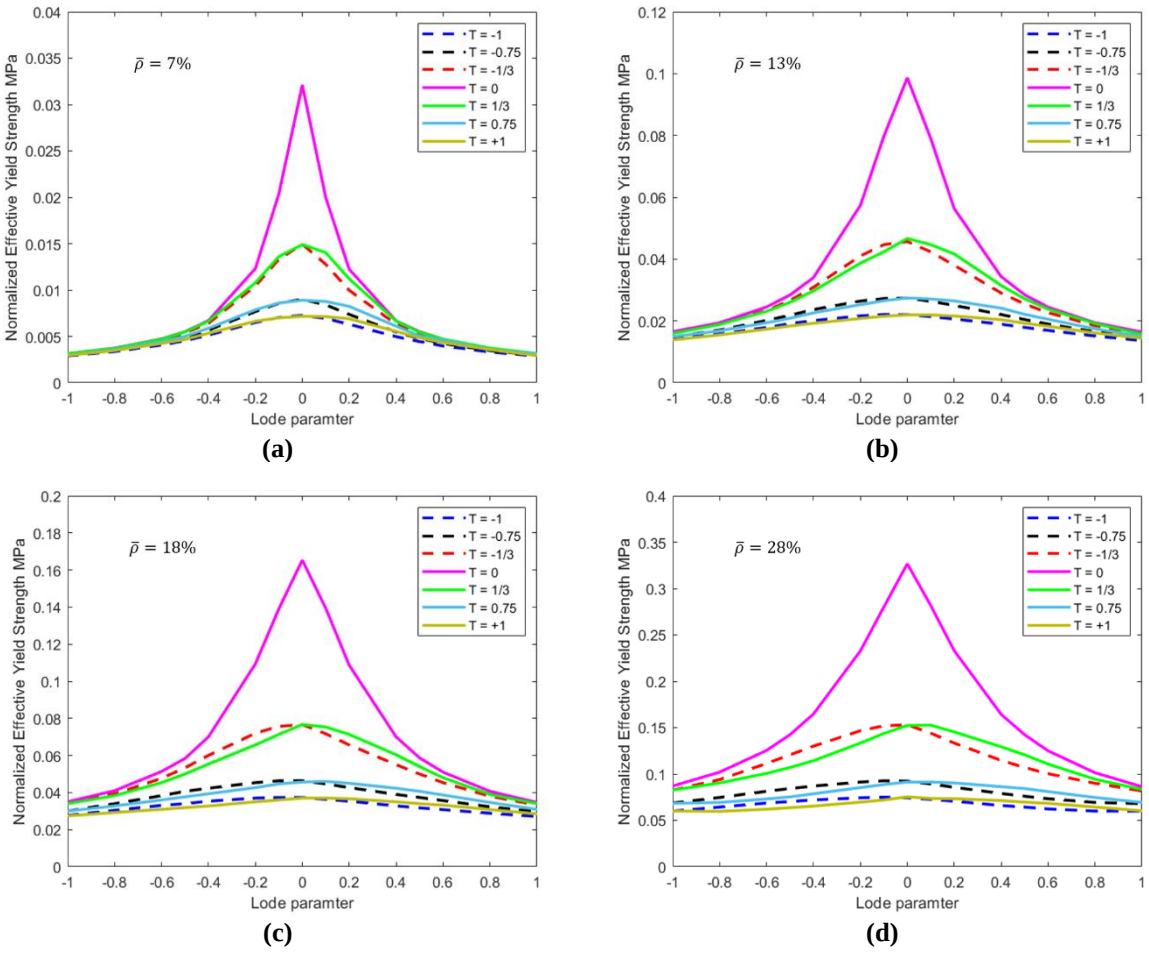

Figure 4: Normalized yield strength versus Lode parameter at constant stress triaxiality values for $\bar{\rho}$ = (a) 7%, (b) 13%, (c) 18%, (d) 28%

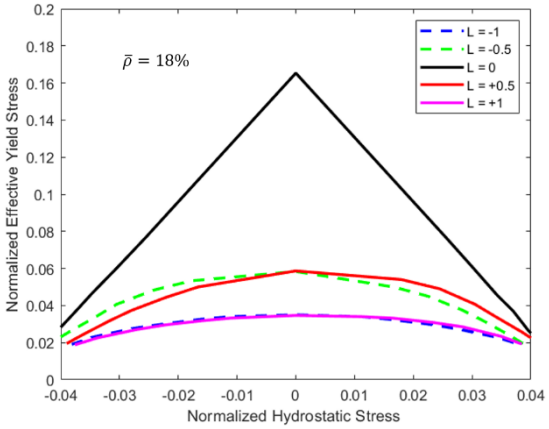

Figure 5: Normalized yield strength versus normalized hydrostatic stress at constant Lode values of -1, 0 and +1 for $\bar{\rho}$ = 18%

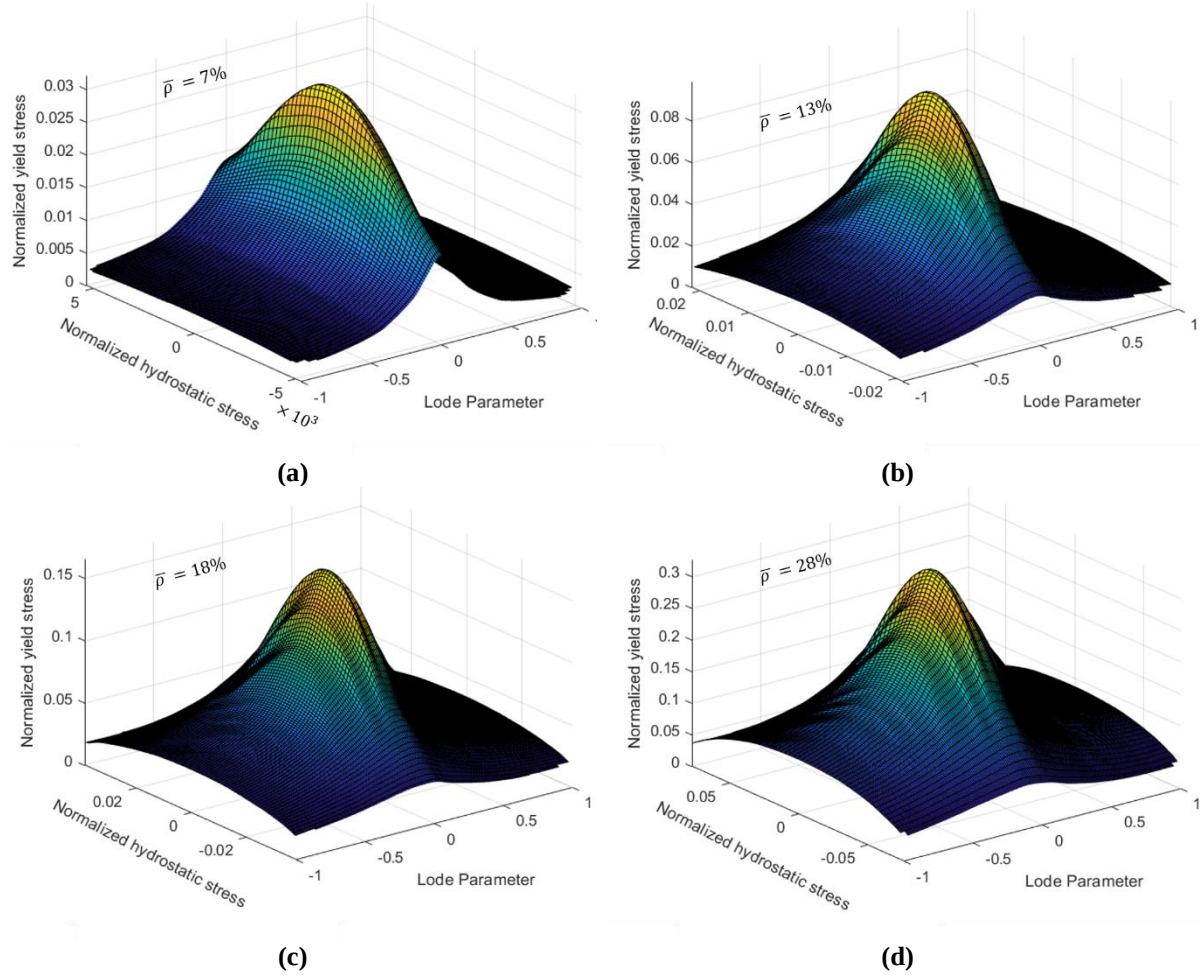

Figure 6: Three-dimensional yield surface of IWP-L for $\bar{\rho}$ of (a) 7%, (b) 13%, (c) 18%, (d) 28%

5 CONCLUSION

In this study, the yield behavior of IWP ligament based TPMS (IWP-L) is numerically investigated through finite element simulations. The effect of the stress triaxiality T and Lode parameter L on the yield strength is investigated for four different relative densities of $\bar{\rho}$ = 7, 13, 18 and 28 %. Periodic boundary conditions are used on one unit cell of IWP-L, which represents the RVE in this study. To capture the macroscopic effective yield strength of the RVE, volume average homogenization is used to get the macroscopic effective true stress and strain behavior of the RVE. Results are presented as a three-dimensional yield surface for each relative density, which show that the highest yield strength occurs at L = 0 and T = 0, with a symmetry across both L and T.

ACKNOWLEDGMENTS

The authors acknowledge the financial support provided by Khalifa University under Award No. RCII-2019-003.

REFERENCES

[1] D.-W. Lee, K. A. Khan and R. K. Abu Al-Rub, "Stiffness and yield strength of architectured foams based on the Schwarz Primitive triply periodic minimal surface," *International Journal of Plasticity,* vol. 95, pp. 1-20, 2017.

[2] O. Al-Ketan and R. K. Abu Al-Rub, "Multifunctional Mechanical Metamaterials Based on Triply Periodic Minimal Surface Lattices," *Advanced Engineering Materials,* 2019.

[3] D. W. Abueidda, R. K. Abu Al-Rub, A. S. Dalaq, D.-W. Lee, K. A. Khan and I. Jasiuk, "Effective conductivities and elastic moduli of novel foams with triply periodic minimal surfaces," *Mechanics of Materials,* vol. 95, pp. 102-115, 2016.

[4] A. H. Schoen, "NASA Technical Report No. D-5541," 1970.

[5] R. K. Abu Al-Rub, D.-W. Lee, K. A. Khan and A. N. Palazotto, "Effective Anisotropic Elastic and Plastic Yield Properties of Periodic Foams Derived from Triply Periodic Schoen's I-WP Minimal Surface," *Journal of Engineering Mechanics,* 2020.

[6] O. Al-Ketan, R. K. Abu Al-Rub and R. Rowshan, "The effect of architecture on the mechanical properties of cellular structures based on the IWP minimal surface," *Journal of Materials Research,* 2018.

[7] O. Al-Ketan, R. Rezgui, R. Rowshan, H. Du, N. X. Fang and R. K. Abu Al-Rub, "Microarchitected Stretching-Dominated Mechanical Metamaterials with Minimal Surface Topologies," *Advanced Engineering Materials,* vol. 20, 2018.

[8] V. Deshpande and N. Fleck, "Isotropic constitutive models for metallic foams," *Journal of the Mechanics and Physics of Solids,* pp. 1253-1283, 2000.

[9] D. L. S. McElwain, A. P. Roberts and A. H. Wilkins, "Yield Functions for PorousMaterials with Cubic Symmetry Using Different Definitions of Yield," *Advanced Engineering Materials,* vol. 8, 2006.

[10] I. Basroum and J. Faleskog, "Rupture mechanisms in combined tension and shear-Experiments," *International Journal of Solids and Structures,* vol. 44, pp. 1768-1786, 2007.

[11] N. Baghous and I. Barsoum, "Effect of Material Strength on Ductile Failure of Steel in Pressure Vessel Design," *Journal of Pressure Vessel Technology,* vol. 143, 2021.

[12] R. K. Abu Al-Rub and O. Al-Ketan, "MSLattice: a free software for generating uniform and graded lattices based on triply periodic minimal surfaces," *Material Design & Processing Communications,* 2020.

[13] HyperMesh, *CAE Altair Hyperworks,* Troy MI, United States: Altair Engineering, Inc..

[14] ABAQUS, "Abaqus Analysis User's Manual (2019)," 2019.

[15] T. 3. E. C. "Micromechanics Plugin For Abaqus/CAE Version 1.16," *Dassault Systemes,* 2020.

[16] I. Barsoum and J. Faleskog, "Rupture mechanisms in combined tension and shear - Micromechanics," *International Journal of Solids and Structures,* vol. 44, pp. 5481-5498, 2007.

[17] K. A. Khan and R. K. Abu Al-Rub, "Time dependent response of architectured Neovius foams," *International Journal of Mechanical Sciences*, vol. 126, pp. 106-119, 2017.